Fragmentation of positronium in collision with He atoms: A classical theoretical approach

L. Sarkadi*

Institute of Nuclear Research of the Hungarian Academy of Sciences (ATOMKI), H-4001 Debrecen, P.O. Box 51, Hungary

(Received 15 January 2003; published 10 September 2003)

The classical trajectory Monte Carlo method was applied to the description of the fragmentation of the positronium (Ps) in collision with He atoms. The collision system was simplified to a three-body system consisting of the electron and the positron of the Ps, as well as the He atom that was considered as a structureless particle. The interaction of the e^- and e^+ with the He was approximated by a static, fully screened Coulomb potential. The calculations were carried out for collision energies 13, 18, 25, and 33 eV. The obtained total break-up cross sections and the longitudinal energy distributions of the emitted positrons were compared with the recent experimental results of Armitage *et al.* [Phys. Rev. Lett. **89**, 173402 (2002)]. The present theory overestimates the measured cross sections by a factor of 1.6–2.5, but it correctly reproduces the peak found by Armitage *et al.* in the positron spectra at about half of the residual Ps energy.

DOI: 10.1103/PhysRevA.68.032706 PACS number(s): 34.10.+x, 36.10.Dr

I. INTRODUCTION

Recently Armitage *et al.* [1] reported the first measurement of the absolute breakup cross sections for the fragmentation of the positronium (Ps) in collision with He atoms in the energy range between 13 and 33 eV. In addition to the measurement of total cross sections, they determined also the longitudinal energy distributions of the emitted positrons. A remarkable feature of the obtained positron spectra is a peak appearing just below 50% of the residual Ps energy ($E_{\rm res} = E_{\rm Ps} - 6.8$ eV). The peak was interpreted as an analogy of the *electron loss to the continuum* (ELC) peak appearing in the energy spectrum of the electrons ejected in the forward direction in ion-atom (atom-atom) collisions. In the latter collisions the cusp-shaped peak is centered at an energy that corresponds to $v_e = v_p$ (here v_e and v_p are the velocities of the electron and projectile, respectively), i.e., the peak is formed by those electrons that travel together with the projectile.

Because of the large similarity between the positron emission following the collisional fragmentation of the Ps and the ELC process, in the following we briefly summarize the main properties of the cusp-electron emission in atomic collisions.

The above-mentioned ELC process may take place when the projectile ion (atom) has bound electron(s). During the collision the projectile may lose its electron(s) with a small kinetic energy as a result of ionization by the target atom. The electrons originating from the projectile are centered around $v_e = v_p$ in the spectrum measured at forward angles. An other related process leading to a cusp in the electron spectrum is a special kind of ionization of the target by the projectile, called *electron capture to the continuum* (ECC). ECC can be viewed as a continuation of the electron capture into high-lying bound states (Rydberg states) of the projectile over the ionization threshold.

The phenomenon of the electron cusp has received much attention in the physics of energetic ion-atom collisions since its discovery [2]. The great interest is explained by its properties of fundamental importance. Both ELC and ECC lead to the population of the low-energy continuum states around the projectile, i.e., the formation of the cusp is a *threshold* phenomenon [3,4] which is governed by the Wigner threshold law [5]. Another general feature of the cusp is that it is a result of final-state interaction between the emitted electron and the outgoing projectile (see, e.g., Ref. [6]). The theoretical description of the cusp is a great challenge. The properties of the peak (intensity, width, asymmetry, etc.) are strongly affected by *three-body* effects due to the interactions between the three collision fragments (electron, target, and projectile) in the outgoing phase of the collision [7].

For collisions involving positrons, the first pioneering experimental study of the cusp phenomenon was carried out by Kövér and Laricchia [8]. These authors bombarded a molecular hydrogen target with 100-eV positrons, and detected the scattered positrons and the ejected electrons in coincidence. The observation angle for both particles was 0°. A broad peak appearing in the coincident energy spectrum of the electrons provided clear evidence for the existence of the electron capture to the continuum states of the positron projectile. (More correctly, in this case one should call this process as ''mutual capture of the electron and positron into each other's continuum states.'') The observation was followed by several theoretical investigations [9–12]. The theoretical interest towards the positron-induced ECC can be explained by the fact that the kinematics of the collision for positron projectile is completely different compared to that of the heavy-particle projectile. For ion (atom) impact the deflection of the projectile is negligibly small, and therefore, the ECC events are concentrated around 0°. Furthermore, the energy loss of the projectile is also negligible in this case. This leads to a pronounced cusp at $v_e = v_p$ in the direction of the incident beam. On the contrary, for positron impact the kinematics is much more complicated, the projectile scatters to large angles, and its energy loss is not negligible. The resulting cusp is not so sharp, and it is distributed over a large angular range. This means that for the theoretical description of the positron-induced ECC the inclusion of the full three-body kinematics is even more crucial than for heavy particles.

In the experiment of Kövér and Laricchia [8], the ECC

*Email address: sarkadil@atomki.hu

peak for positron impact was found to be centered in the electron spectrum also at about half of the residual energy, $E_{res}/2$ (in this case $E_{res}=E_{e^+}-I$, where I is the ionization energy of the target). This suggests a similarity between the positron-induced ECC process and the formation of the positron peak observed by Armitage *et al.* [1] in the collisional fragmentation of the Ps. Searching for a common feature of the regarded collisions, we may assume that in both cases highly excited bound states of the Ps can be formed: for positron impact the positron may capture a target electron into states of high principal quantum number, while for the collisions of the Ps with atoms the excitation of the Ps may lead to such states. Since there is a smooth transition between the bound and continuum states, we may also assume capture or excitation to *unbound* Ps states. If the energy of such states is small [with respect to the center of mass (c.m.) of the Ps], then the relative motion of the e^- and e^+ is primarily determined by their mutual interaction, and it is less affected by the field of the target—we may speak about the continuum states of the Ps in this sense. The small relative energy of the e^- and e^+ means that the two particles share the residual energy equally, i.e., their kinetic energy with respect to the target is $E_{res}/2$.

Armitage *et al.* [1] compared their measured total breakup cross sections with the predictions of two theories: The model of Biswas and Adhikari [13] based on the Born approximation, and the coupled-state calculations carried out by Blackwood *et al.* [14]. Good agreement was found with the latter theory. However, the authors could not compare the obtained longitudinal energy distributions of the emitted positrons with theory, because there were no existing calculations. In this paper we report on a work in which differential properties of the e^- and e^+ emission following the collisional breakup of the Ps have been determined by using a classical theoretical approach, namely, the *classical trajectory Monte Carlo* (CTMC) method.

II. THEORY

In the description of the collisions of the Ps with He atoms we considered the He atoms as structureless particles, i.e., we assumed that the fragmentation of the Ps is primarily determined by the dynamics of three particles: the e^- and e^+ of the Ps and the ground-state He atom. This simplification (that can be justified by the ''compact'' character of the He atom due to its large first excitation energy and ionization potential) also means that we neglect any inelastic effects due to virtual and real excitations of the He target during the fragmentation. As a further consequence of considering the target as a structureless particle is that the exchange interaction between the electrons of the He and the electron of the Ps cannot be included in the model.

In a Ps-centered reference frame the fragmentation of the Ps due to its collisions with He atoms can be viewed as the ionization of the Ps atom by the impact of He projectiles. The description of the breakup of the Ps in the *reversed* collision system He→Ps (instead of considering the direct collision system Ps→He) has the advantage that in this case the process is an analogy of the ionization of atoms by heavy-particle impact. On the basis of this analogy, one can treat the problem of the collisional break-up of the Ps by using the theoretical methods worked out for the description of the heavy-particle-induced ionization of atoms. Let us consider the simplest case, the ionization of the H atom by a structureless heavy particle. If in a model developed for the latter process the three-body kinematics is taken into account exactly, one can use the same model for the calculations of ionization cross sections for the He→Ps system, simply by replacing the H target atom by the Ps. Performing such calculations, final breakup cross sections for the Ps→He collisions are obtained by transforming the ionization cross sections to the projectile-centered reference system.

In this work we used the three-dimensional, three-body version of the CTMC method [15,16] for the description of the He→Ps collision. Details of our procedure applying the CTMC method to the treatment of various atomic collision-processes can be found in previous works [17–22], therefore, here we summarize only the main points of the theory. The method is based on a numerical solution of Newton's classical equations of motion under randomly chosen initial conditions. From the point of view of the present investigations CTMC has the particularly important advantage that the three-body dynamics of the collision is exactly treated by the method.

Since our CTMC computer code is applicable to particles of arbitrary masses, we could use it for the Ps target atom without any modifications. We note that the present studied problem of the energy distribution of the emitted positrons following the fragmentation of the Ps is related to the problem of the momentum distribution of the *recoil ions* in atomic collisions: The role of the recoil ion following the ionization of the Ps is played by the positron. In a previous work [22] we successfully applied CTMC to the interpretation of the results of a recoil-ion experiment [23].

The equations of motion were solved with the following interactions between the three particles. The e^- and e^+ of the Ps interacted through a pure, attractive Coulomb force. Concerning the interaction of the e^- and e^+ with the structureless He projectile, we expressed it in the form of a static, fully screened Coulomb potential (in atomic units):

$$V(r)=q\frac{Z_P(r)}{r}. \tag{1}$$

Here $q=1$ or -1 for interaction with the e^+ or e^-, respectively. The screened nuclear charge $Z_P(r)$ of the neutral He atom was deduced from the model potential developed by Green *et al.* [24] on the basis of Hartree-Fock calculations. This latter potential determines the interaction energy of an electron in an atom or ion, and has the following general form:

$$V(r)=q\frac{Z-(N-1)[1-\Omega(r)]}{r}, \tag{2}$$

where N is the number of the electrons in the atom (ion), Z is the nuclear charge, and

$$\Omega(r)=\{(\eta/\xi)[\exp(\xi r)-1]+1\}^{-1}. \quad (3)$$

η and ξ are parameters determined by energy minimization. The interaction energy between the e^- and the neutral He atom can be obtained by applying Eq. (2) to the $(e^-+\mathrm{He})$ system, i.e., for $Z=2$ and $N=3$. This yields

$$V(r)=q\frac{2\Omega(r)}{r}. \quad (4)$$

Comparing Eqs. (1) and (4), we have

$$Z_\mathrm{P}(r)=2\,\Omega(r). \quad (5)$$

From Eq. (3) one can see that $Z_\mathrm{P}(r)$ takes the nuclear charge of the He at the origin, $Z_\mathrm{P}(0)=2$. For $r\gg r_c\equiv 1/\xi$ the screened nuclear charge vanishes exponentially, $Z_\mathrm{P}(r)\propto\exp(-\xi r)$, i.e., the potential defined by Eq. (1) has a short interaction range. In our calculations we used η and ξ values given by Garvey *et al.* [25], $\eta=1.067$ and $\xi=1.188$.

We note that the use of a potential of the same form for the e^- and e^+ is probably a rough approximation. In addition to the electron-electron exchange effect, in our model we also neglect the dynamical polarization of the He atom. This latter effect is expected to be different for the e^- and e^+, leading to a further asymmetry in the strength of the interaction. However, we emphasize the model character of the present calculations. Equation (1) with the screened nuclear charge (5) gives account of the main features of the interaction of the e^- and e^+ with the He atom: The two interactions are of opposite sign, close to the nucleus of the atom they are Coulombic, and far from the nucleus they vanish exponentially.

Concerning the choice of the random initial parameters, we followed the general procedure proposed by Reinhold and Falcón [26]. The integration of the motion was started at a distance of about 100 a.u. between the projectile and the c.m. of the Ps. After the collision the check of the conditions for the exit channels (excitation, ionization) was made also at a separation of about 100 a.u. To fully account for the post-collision interaction effects, in the ionization channel the integration of the trajectories was continued over distances of 10^5 a.u.

The number of collision events considered in the simulation at a given incident Ps energy was typically 10^5. For the differential analysis of the fragmentation process (dependence on the emission energy and angle of the e^- and e^+) 10^6 trajectories were required, in order to achieve a satisfactory statistical accuracy. In CTMC the transformation of the results from the reversed collision system to the direct one is simple: One has to perform a velocity transformation on the trajectories.

By using the standard procedure of CTMC, from the transformed trajectory data we determined the total Ps breakup cross sections

$$\sigma\approx 2\pi\frac{b_\mathrm{max}}{N_\mathrm{traj}}\sum_j b_j^{(i)}, \quad (6)$$

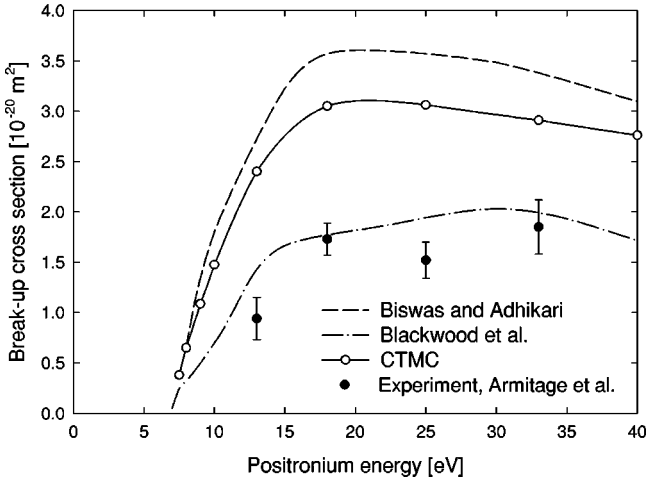

FIG. 1. Total breakup cross sections for Ps-He collisions as a function of the Ps energy. Experimental data: full circles, Armitage *et al.* [1]. Theories: solid line, CTMC (this work); dashed curve, Born approximation (Biswas and Adhikari [13]); dash-dotted line, coupled-state theory (Blackwood *et al.* [14]).

cross sections differential with respect to the longitudinal energy of the emitted positrons,

$$\frac{d\sigma}{dE_z}\approx 2\pi\frac{b_\mathrm{max}}{N_\mathrm{traj}\Delta E_z}\sum_j b_j^{(i)}, \quad (7)$$

and cross sections differential with respect to the energy and angle of the emitted e^- and e^+,

$$\frac{d^2\sigma}{dE\,d\Omega}\approx\frac{b_\mathrm{max}}{N_\mathrm{traj}\Delta E(\cos\vartheta_\mathrm{min}-\cos\vartheta_\mathrm{max})}\sum_j b_j^{(i)}. \quad (8)$$

In the above expressions N_traj is the total number of trajectories calculated in the impact-parameter range $(0,b_\mathrm{max})$. $b_j^{(i)}$ is the actual impact parameter when the criterion of the ionization is fulfilled—in Eq. (6) without any further condition, in Eq. (7) with the condition that the longitudinal positron energy is between E_z and $E_z+\Delta E_z$ (E_z is defined as $\frac{1}{2}v_z^2$, where v_z is the projection of the velocity of the positron onto the direction of the incident Ps beam), and in Eq. (8) with the condition that the e^- or e^+ is emitted with an energy and a polar angle that lie in the intervals $(E,E+\Delta E)$ and $(\vartheta_\mathrm{min},\vartheta_\mathrm{max})$, respectively.

III. RESULTS AND DISCUSSION

In Fig. 1 the total breakup cross sections obtained by the present CTMC calculations for Ps→He collisions are compared with the experimental data and other theoretical predictions. The present theory overestimates the measured data by a factor between 1.6 and 2.5, depending on the Ps energy. Interestingly, the shape of the CTMC curve is very similar to that obtained by Biswas and Adhikari [13] in the Born approximation: Both theories predict the maximum of the breakup cross section to occur at $E_\mathrm{Ps}\approx 20$ eV, in disagreement with the coupled-state theory of Blackwood *et al.* [14]

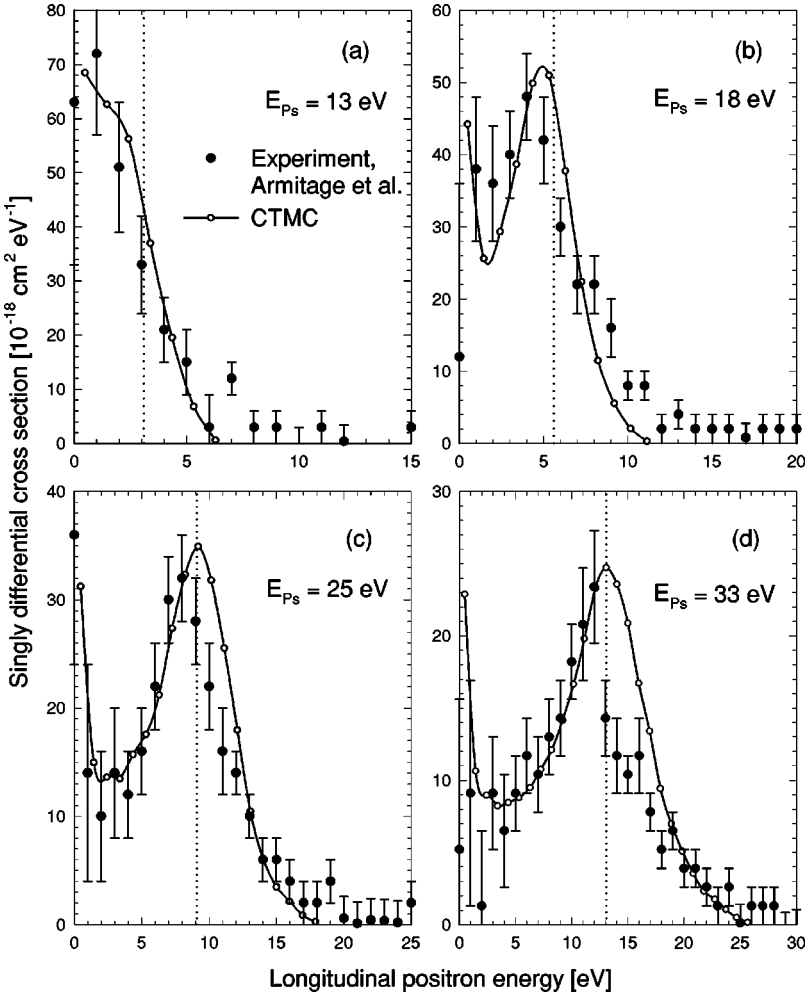

FIG. 2. Longitudinal energy distributions of the positrons emitted in Ps-He collisions for $E_{\mathrm{Ps}}=13$, 18, 25, and 33 eV. The experimental data (full circles, Armitage *et al.* [1]) are normalized to the maxima of the theoretical curves calculated by the present CTMC model. The normalization factors are 3, 2, 2, and 1.3 for $E_{\mathrm{Ps}}=13$, 18, 25, and 33 eV, respectively. The vertical dotted line shows the expected peak position $E_{\mathrm{res}}/2$.

that shows a maximum at $E_{\mathrm{Ps}}\approx 32$ eV. The experiment supports the latter theory.

In Fig. 2 the longitudinal energy distributions of the positrons are compared with the corresponding experimental data for Ps energies 13, 18, 25, and 33 eV. Since we are mainly interested in the shapes of the distributions, in the figure the experimental data are normalized to the CTMC cross sections at the maxima of the distributions. CTMC seems to give a correct description of the measured positron spectra. It reproduces the peak occurring at $E_{\mathrm{res}}/2$, supporting in this way the mechanism similar to ELC in atomic collisions. The width and asymmetry of the peak predicted by CTMC show a reasonable agreement with the experiment. A remarkable achievement of this simple model is that in the calculated distributions one can observe the same tendency as in the measured ones: With decreasing collision energy the peak becomes less pronounced and even disappears at $E_{\mathrm{Ps}}=13$ eV.

One can see from Fig. 2 that the measured peaks show a shift from the expected position to lower e^+ energies. The shift can be understood considering that these longitudinal energy spectra are integrated distributions over the e^+ emission angle, and assuming that the angular distribution is not sharply peaked at 0°. Armitage *et al.* [1] estimated from the observed shifts that the breakup positrons are probably released within an angle of 20° at higher Ps energies.

The CTMC results show also a shift of the peak at $E_{\mathrm{Ps}}=18$ eV, but for $E_{\mathrm{Ps}}=25$ and 33 eV one cannot observe any shift of the calculated peaks. However, there is another source of the shift of the peak position that was not considered in the calculations. The experiment was carried out by a Ps beam having an energy spread of about 5 eV [full width at half maximum (FWHM)]. The energy spread of the beam gives rise not only to a broadening of the peak, but also to a shift. This is demonstrated in Fig. 3 by our model calculations carried out for the case of the 18 eV beam energy. We simulated the experimental Ps beam consisting of nine monoenergetic components with energies $E_{\mathrm{Ps}}=14,15,\ldots,22$ eV. We assumed a Gaussian intensity distribution of the components with a maximum energy of 18 eV and a FWHM of 5 eV. We ran the CTMC code for each Ps energy. The obtained longitudinal positron energy distributions are displayed in the upper part of Fig. 3. The lower part of the figure shows the average of the spectra calculated with the Gaussian intensity weights of the beam components. The convolution with the energy profile of the Ps beam leads to a further shift of the peak (in addition to the effect of the finite angular distribution) due to the fact that the low-energy components contribute to the sum with larger intensities than the high-energy ones. According to Fig. 3, the inclusion of the

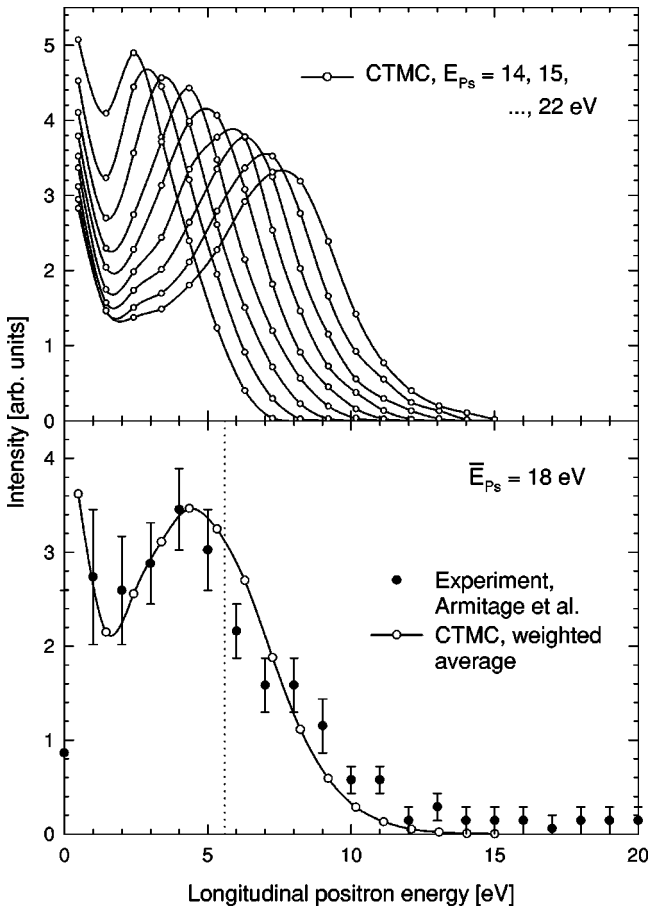

FIG. 3. The effect of the energy spread of the Ps beam on the longitudinal energy distribution of the positrons ejected in 18 eV Ps-He collisions. Upper part: distributions calculated by the present CTMC model for $E_{Ps}=14,15,\ldots,22$ eV. Lower part: solid line, weighted average of the calculated distributions; full circles, experimental data of Armitage *et al.* [1].

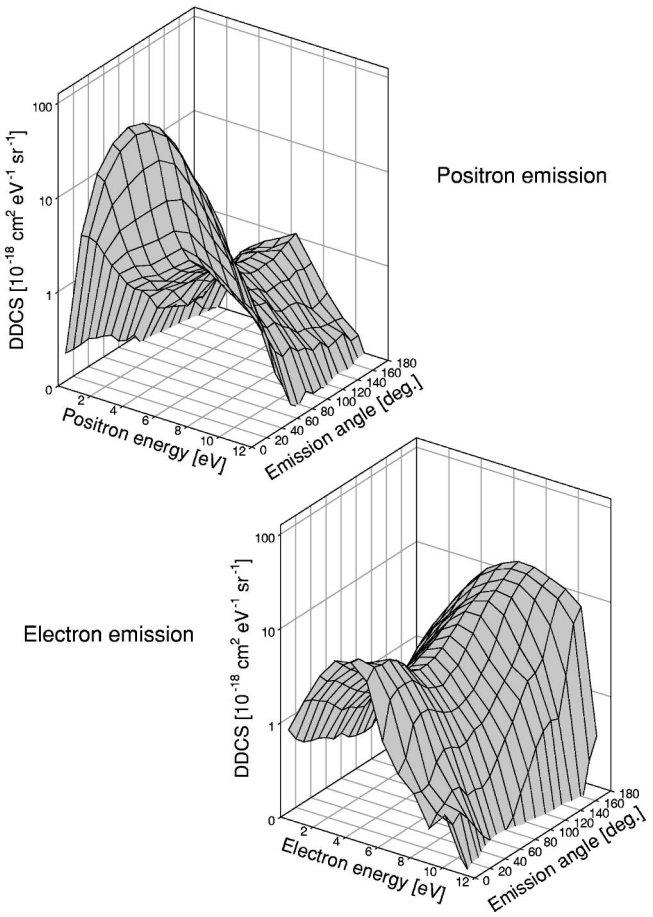

FIG. 4. The dependence of the DDCS on the emission energy and angle of the positrons (upper part) and the electrons (lower part) for 18 eV Ps-He collisions (present CTMC results).

energy spread of the Ps beam in the calculations resulted in a significant improvement in the description of the measured distribution.

For a better understanding of the collisional fragmentation of the Ps, in Fig. 4 we plotted the doubly differential cross section (DDCS) values obtained by CTMC for the e^+ and e^- emission in a three-dimensional logarithmic representation. The incident Ps energy is 18 eV. The distribution for both particles has the form of saddle surface, having one minimum around 90° and two maxima at 0° and 180°. The e^+ emission is confined to a small angular range in the forward direction. The DDCS values steeply decrease above 20°, in agreement with the estimation of Armitage *et al.* [1]. The peak at 180° is very small, the probability of the e^+ emission in the backward direction is smaller by two orders of magnitude than in the forward direction. On the contrary, for e^- the backward emission is more enhanced, though the directional asymmetry is not so large in this case: Along the ridge of the distribution the DDCS values depend only weakly on the emission angle.

On the basis of Fig. 4 we may outline the following picture of the Ps fragmentation. The collision of the Ps with the He can be viewed as a scattering of quasifree e^- and e^+ on the target atom. The different energy and angular dependence of the DDCS seen in the figure for the e^- and e^+ emissions indicates that the two particles scatter differently. The dominant scattering of the e^+ in the forward direction means that this particle is emitted via *soft* binary collisions with the target characterized by small momentum transfer. The dependence on the emission energy is mainly determined by the initial velocity distribution (the Compton profile) of the e^+ in the Ps. On the contrary, the distribution seen in Fig. 4 for the e^- emission can be attributed to *hard* binary collisions of the e^- with the target in which the large momentum transfer leads to large-angle scatterings. Particularly, the peak at 180° can be explained as the result of a backscattering of the quasifree electrons from the He atom. The soft collision of the e^+ and the hard collision of the e^- occurring simultaneously with the target mean that the fragmentation of the Ps takes place predominantly via the interaction of the e^- with the He atom, and in the process the e^+ plays only the role of a spectator particle.

The question arises: Why the e^- and e^+ behave differently in the fragmentation process? A possible answer to this question is as follows. In the range of the regarded impact energies the collision is adiabatic. When the Ps approaches

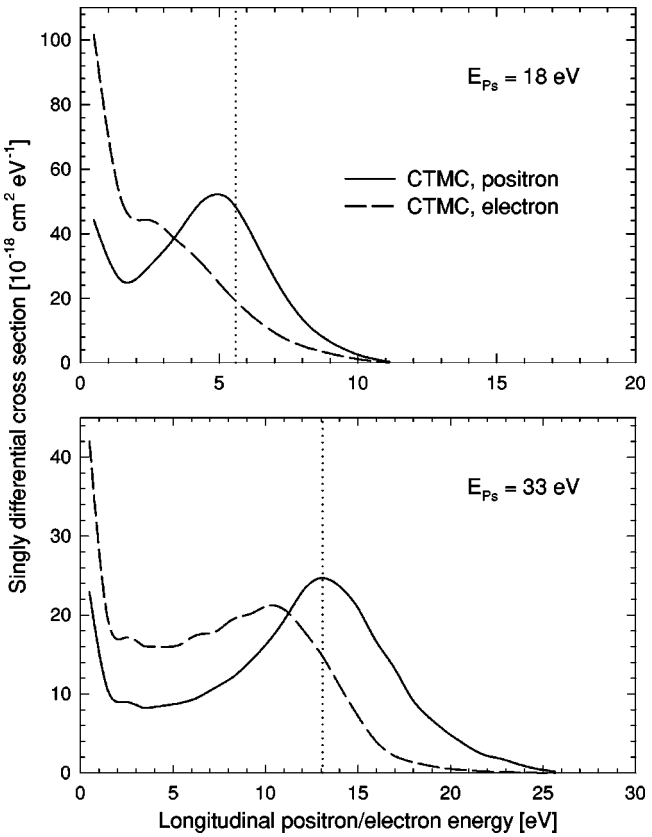

FIG. 5. Calculated longitudinal energy distributions of the positrons (solid line) and electrons (dashed line) ejected in Ps-He collisions for $E_{\mathrm{Ps}}=18$ eV (upper part) and 33 eV (lower part). The vertical dotted line shows the expected peak position $E_{\mathrm{res}}/2$.

the target, the motion of the e^- and e^+ is distorted by the increasing interaction between these particles and the He atom. The Ps becomes polarized: the e^+ is repelled and the e^- is attracted by the screened Coulomb field of the target. As a result of the polarization, on average the e^- stays closer to the target nucleus than the e^+, i.e., the probability that the e^- undergoes hard collisions with the He atom increases. This means that the breakup of the Ps takes place dominantly via the impulsive ejection of the e^-. The e^+ interacts with the target mainly in distant, soft collisions, which leads to breakup with smaller probability.

A decisive check of the present CTMC model would be the measurement of the longitudinal energy distribution of the emitted electrons, in the same way as it was done for the positron emission in the experiment by Armitage *et al.* [1]. CTMC predicts a significant difference between the distributions belonging to the e^- and e^+ emissions. This is shown in Fig. 5 where we plotted our CTMC results for $E_{\mathrm{Ps}}=18$ and 33 eV. In the longitudinal energy distributions of the electrons one can also observe a peak, but it is less pronounced and significantly shifted from $E_{\mathrm{res}}/2$. For $E_{\mathrm{Ps}}=18$ eV the peak is only a small hump sitting on a steep background of low-energy electrons. The enhancement of the low-energy part of the spectrum (in comparison with the positrons) is due to the enhanced electron emission at angles around 90° (see Fig. 4), considering that the longitudinal velocity component of those electrons is close to zero. The small peak can be explained by the maxima of the DDCS appearing at 0° and 180°. The dominant contribution to the peak comes from the backward electron emission.

For $E_{\mathrm{Ps}}=33$ eV the difference between the distributions for the two particles is smaller. One may expect that with increasing Ps energy the $e^- - e^+$ difference disappears completely. This means that the energy and angular dependence of the DDCS seen in Fig. 4 for the e^- emission will probably be similar to that seen for the e^+ emission. For high impact energies the picture of quasifree scattering of the e^- and e^+ on the He target is better founded. The polarization of the Ps by the target is negligible in this case, both the e^- and e^+ are expected to be released predominantly in the forward direction with mean energy $E_{\mathrm{res}}/2$ and with an energy distribution determined mainly by the initial velocity distribution (the Compton profile) of the particles in the Ps.

As it was discussed in Sec. II, one of the most questionable approximations applied in the present model is the use of the potential given in Eq. (1) for the interaction of the e^- and e^+ with the He target atom. The detailed study of this problem is outside the scope of the present work. Nevertheless, an interesting question emerges about as how sensitively the CTMC results depend on the parameters of the potential. One expects a strong dependence on the ξ parameter that determines the interaction length by the relationship $r_c=1/\xi$, therefore we checked the sensitivity of the model on this parameter. We changed the value of ξ from 1.188 to 2 (i.e., reduced the interaction length r_c from 0.841 to 0.5 a.u.), and repeated the calculations for $E_{\mathrm{Ps}}=18$ and 33 eV.

As a result of using a shorter interaction length the cross sections reduced significantly, as is seen in Fig. 6 where longitudinal energy distributions obtained from the calculations with $r_c=0.841$ and 0.5 a.u. are plotted. In parts (a) and (b) of the figure (positron emission) we also plotted the experimental data, but now without normalizing them to the theoretical cross sections. Comparing the distributions belonging to $r_c=0.841$ and 0.5 a.u., one may conclude that the main features predicted by CTMC for the fragmentation of the Ps remain the same when the interaction length is changed. For 33 eV impact energy the shapes of the distributions are almost identical. The shapes of the spectra are also similar for $E_{\mathrm{Ps}}=18$ eV, although the peak in the positron spectrum obtained for $r_c=0.5$ a.u. is less pronounced and shows a larger shift compared to the peak belonging to the longer interaction length. The same behavior can be observed for the small hump in the electron spectrum at 18 eV impact energy.

The use of a shorter interaction length resulted in a considerable improvement of the present model regarding the reproduction of the *absolute* values of the measured singly differential cross sections. This indicates that for the treatment of the Ps + He collisions, one probably cannot use η and ξ values that were determined by atomic structure calculations. However, the uncertainty of the calculated cross sections is large due to the applied approximations (classical treatment, three-body approximation, neglect of the exchange effect, the dynamical polarization of the He target, etc.). Therefore, from the present CTMC results it is hard to draw any firm conclusions on the potential.

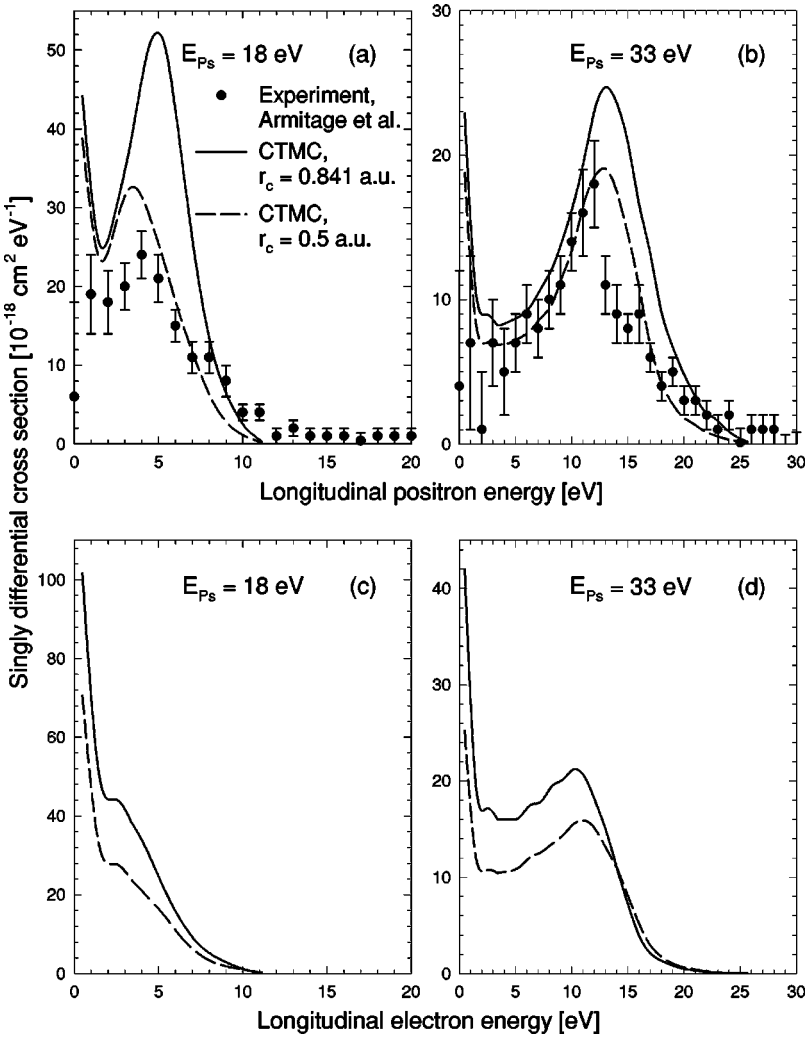

FIG. 6. Longitudinal energy distributions of the positrons [panels (a) and (b)] and electrons [panels (c) and (d)] ejected in Ps-He collisions for $E_{\mathrm{Ps}}=18$ eV [panels (a) and (c)] and 33 eV [panels (b) and (d)]. The curves are results of CTMC calculations carried out with different values of the interaction length for the potential given by Eq. (1): solid line, $r_c=0.841$ a.u.; dashed line, $r_c=0.5$ a.u. For positron emission the experimental data of Armitage *et al.* [1] are also plotted (full circles).

Finally, we briefly discuss the limitations of the present model. In the past three decades a considerable effort has been devoted to clarify the background and the domain of validity of the CTMC method in the field of ion-atom collisions (see, e.g., Refs. [27–30]). It is a commonly accepted view that CTMC is particularly suitable for the treatment of the collisions in the range of intermediate velocities ($v \sim 1$ a.u.), i.e., in the case of large perturbations. The appropriate quantum-mechanical description in this velocity range is the coupled-channel method. This latter approach is, however, limited in practice by basis-set incompletness. On the other hand, below and above the ionization maximum the quantum-mechanical perturbation theories give a better description than CTMC in those cases when the ionization of an atom is induced by a small perturbation. For a given collision system the strength of the perturbation can be characterized by the transferred momentum and the impact parameter. Typically, for weak perturbations the ionization process is characterized by small momentum transfers and/or large impact parameters. Under such conditions the ionization takes place predominantly via nonclassical dipolelike transitions, consequently, for weak perturbations CTMC underestimates the ionization cross sections [29].

Concerning the present study, the velocity range is ideal for the use of CTMC. The impact parameters which give the dominant contribution to the breakup cross section of the Ps are typically smaller than (or comparable to) the Bohr radius of the Ps. The perturbation is large, in the impulsive collisions large amount of momentum is transferred on average to the electron (positron). Accordingly, the application of CTMC is well justified.

A serious limitation of the present model is that it is a three-body approximation to the full, five-body collision problem. The improvement of the model by including the electrons of the He target in the calculations would not be an easy task due to the fact that multielectron atoms are classically unstable with respect to autoionization (see, e.g., Ref. [31]). Regarding also the nonclassical effect of the electron-electron exchange, a complete description of the process is expected only by quantum-mechanical calculations. In this respect it is interesting to compare the present CTMC model with the coupled-state theory of Blackwood *et al.* [14]. The latter theory is a complete description in that sense that it includes all the five particles and all interactions between them. The expansion of the collision wave function contains 22 Ps states and one He state. Among the Ps states there are 19 pseudostates for the representation of the continuum of the Ps. The description of He by one state (the 1*s* state)

implies that—like in our model—the excitation and ionization of the target (real or virtual) are excluded in the calculations. Blackwood *et al.* [14] used their model for the calculation of *total* (integrated) scattering cross sections. According to Fig. 1, the predictions of the coupled-state model for the total ionization cross section are in good agreement with the experiment. However, Blackwood *et al.* [14] did not determine *differential* cross sections for the fragmentation of the Ps, therefore one cannot compare the performance of the two models in reproducing the longitudinal energy distributions of the positrons measured by Armitage *et al.* [1]. It is a question whether the model of Blackwood *et al.* [14] is suitable for the calculation of differential cross sections. In ion-atom collisions it has been realized recently (see, e.g., the review by Kirchner *et al.* [32]) that in coupled-states calculations the representation of the continuum by pseudostates leads to spurious oscillations of the excitation amplitudes. Furthermore, it is a further question whether the number of the pseudostates used by Blackwood *et al.* [14] is sufficient to reproduce the rapid changes of the DDCS found in the present CTMC calculations for the emission of the positrons and electrons (see Fig. 4).

IV. CONCLUSIONS

A three-body version of the CTMC method was applied in the present work to interpret the experimental data obtained by Armitage *et al.* [1] for the fragmentation of the Ps in collisions with He atoms. The calculations were carried out for collision energies 13, 18, 25, and 33 eV. The model significantly overestimates the total break-up cross sections. At the same time, it correctly reproduces the peak observed in the experimental longitudinal energy distribution of the emitted positrons at $E_{\mathrm{res}}/2$, supporting the idea of a peak formation mechanism similar to ELC in atomic collisions.

The dependence of the e^- and e^+ ejection on the emission energy and angle was also investigated. A strong e^--e^+ asymmetry was found for the doubly differential cross sections at low impact energies. This behavior was explained by the polarization of the Ps atom in the incoming phase of the collision. The asymmetry is expected to diminish at high impact energies.

According to the calculations, a significant $e^- - e^+$ difference is expected to occur also in the longitudinal energy distributions of the ejected particles. CTMC predicts a peak also in the electron spectrum, but it is less pronounced and shows a larger shift from $E_{\mathrm{res}}/2$ than the corresponding peak in the positron spectrum. An experiment is suggested in which the longitudinal energy distribution of the electrons emitted in the fragmentation of the Ps would be measured.

ACKNOWLEDGMENTS

The author is indebted to Gaetana Laricchia for clarifying details of the experiment and providing measured data, and thanks Raúl O. Barrachina for helpful comments. This work was supported by the Hungarian Scientific Research Foundation (OTKA, Grant No. T031833) and the National Information Infrastructure Program (NIIF).

[1] S. Armitage, D.E. Leslie, A.J. Garner, and G. Laricchia, Phys. Rev. Lett. **89**, 173402 (2002).
[2] G.B. Crooks and M.E. Rudd, Phys. Rev. Lett. **25**, 1599 (1970).
[3] J. Macek, Phys. Rev. A **1**, 235 (1970).
[4] M.E. Rudd and J. Macek, Case Stud. At. Phys. **3**, 48 (1972).
[5] E.P. Wigner, Phys. Rev. **73**, 1002 (1948).
[6] R.O. Barrachina, Nucl. Instrum. Methods Phys. Res. B **124**, 198 (1997).
[7] P.D. Fainstein, V.H. Ponce, and R.D. Rivarola, J. Phys. B **24**, 3091 (1991).
[8] Á. Kövér and G. Laricchia, Phys. Rev. Lett. **80**, 5309 (1998).
[9] J. Berakdar, Phys. Rev. Lett. **81**, 1393 (1998).
[10] K. Tőkési and Á. Kövér, J. Phys. B **33**, 3067 (2000).
[11] J. Fiol, V.D. Rodríguez, and R.O. Barrachina, J. Phys. B **34**, 933 (2001).
[12] J. Fiol and R.E. Olson, J. Phys. B **35**, 1173 (2002).
[13] P.K. Biswas and S.K. Adhikari, Phys. Rev. A **59**, 363 (1999).
[14] J.E. Blackwood, C.P. Campbell, M.T. McAlinden, and H.R.J. Walters, Phys. Rev. A **60**, 4454 (1999).
[15] R. Abrines and I.C. Percival, Proc. Phys. Soc. London **88**, 861 (1966).
[16] R.E. Olson and A. Salop, Phys. Rev. A **16**, 531 (1977).
[17] K. Tőkési and T. Mukoyama, Bull. Inst. Chem. Res., Kyoto Univ. **72**, 62 (1994).
[18] K. Tőkési, L. Sarkadi, and T. Mukoyama, J. Phys. B **30**, L123 (1997).
[19] L. Sarkadi, U. Brinkmann, A. Báder, R. Hippler, K. Tőkési, and L. Gulyás, Phys. Rev. A **58**, 296 (1998).
[20] L. Sarkadi, K. Tőkési, and R.O. Barrachina, J. Phys. B **33**, 847 (2000).
[21] L. Sarkadi, L. Lugosi, K. Tőkési, L. Gulyás, and Á. Kövér, J. Phys. B **34**, 4901 (2001).
[22] L. Sarkadi, L. Gulyás, and L. Lugosi, Phys. Rev. A **65**, 052715 (2002).
[23] L. An, Kh. Khayyat, and M. Schultz, Phys. Rev. A **63**, 030703(R) (2001).
[24] A.E.S. Green, D.L. Sellin, and A.S. Zachor, Phys. Rev. **184**, 1 (1969).
[25] R.H. Garvey, C.H. Jackman, and A.E.S. Green, Phys. Rev. A **12**, 1144 (1975).
[26] C.O. Reinhold and C.A. Falcón, Phys. Rev. A **33**, 3859 (1986).
[27] G. Schiwietz and W. Fritsch, J. Phys. B **20**, 5463 (1987).
[28] C.O. Reinhold and C.A. Falcón, J. Phys. B **21**, 1829 (1988).
[29] C.O. Reinhold and J. Burgdörfer, J. Phys. B **26**, 3101 (1993).
[30] S. Keiler, H. Ast, and R.M. Dreizler, J. Phys. B **26**, L737 (1993).
[31] J.S. Cohen, Phys. Rev. A **54**, 573 (1996).
[32] T. Kirchner, H.J. Lüdde, O.J. Kroneisen, and R.M. Dreizler, Nucl. Instrum. Methods Phys. Res. B **154**, 46 (1999).